Evaluation of a SPLUNC1-derived peptide for the treatment of cystic fibrosis lung disease

Shawn T. Terryah,[1] Robert C. Fellner,[1] Saira Ahmad,[1] Patrick J. Moore,[1] Boris Reidel,[1] Juliana I. Sesma,[2] Christine S. Kim,[1] Alaina L. Garland,[1] David W. Scott,[2] Juan R. Sabater,[3] Jerome Carpenter,[1] Scott H. Randell,[1,4] Mehmet Kesimer,[1] William M. Abraham,[3] William J. Arendshorst,[4] and Robert Tarran[1,4]

[1]*Cystic Fibrosis Center/Marsico Lung Institute, The University of North Carolina at Chapel Hill, Chapel Hill, North Carolina;* [2]*Spyryx Biosciences, Durham, North Carolina;* [3]*Department of Research, Mount Sinai Medical Center, Miami Beach, Florida; and* [4]*Cell Biology and Physiology, The University of North Carolina at Chapel Hill, Chapel Hill, North Carolina*

Submitted 12 December 2016; accepted in final form 28 September 2017

Terryah ST, Fellner RC, Ahmad S, Moore PJ, Reidel B, Sesma JI, Kim CS, Garland AL, Scott DW, Sabater JR, Carpenter J, Randell SH, Kesimer M, Abraham WM, Arendshorst WJ, Tarran R. Evaluation of a SPLUNC1-derived peptide for the treatment of cystic fibrosis lung disease. *Am J Physiol Lung Cell Mol Physiol* 314: L192–L205, 2018. First published October 5, 2017; doi:10.1152/ajplung.00546.2016.—In cystic fibrosis (CF) lungs, epithelial Na^+ channel (ENaC) hyperactivity causes a reduction in airway surface liquid volume, leading to decreased mucociliary clearance, chronic bacterial infection, and lung damage. Inhibition of ENaC is an attractive therapeutic option. However, ENaC antagonists have failed clinically because of off-target effects in the kidney. The S18 peptide is a naturally occurring short palate lung and nasal epithelial clone 1 (SPLUNC1)-derived ENaC antagonist that restores airway surface liquid height for up to 24 h in CF human bronchial epithelial cultures. However, its efficacy and safety in vivo are unknown. To interrogate the potential clinical efficacy of S18, we assessed its safety and efficacy using human airway cultures and animal models. S18-mucus interactions were tested using superresolution microscopy, quartz crystal microbalance with dissipation, and confocal microscopy. Human and murine airway cultures were used to measure airway surface liquid height. Off-target effects were assessed in conscious mice and anesthetized rats. Morbidity and mortality were assessed in the β-ENaC-transgenic (Tg) mouse model. Restoration of normal mucus clearance was measured in cystic fibrosis transmembrane conductance regulator inhibitor 172 [CFTR(inh)-172]-challenged sheep. We found that S18 does not interact with mucus and rapidly penetrated dehydrated CF mucus. Compared with amiloride, an early generation ENaC antagonist, S18 displayed a superior ability to slow airway surface liquid absorption, reverse CFTR(inh)-172-induced reduction of mucus transport, and reduce morbidity and mortality in the β-ENaC-Tg mouse, all without inducing any detectable signs of renal toxicity. These data suggest that S18 is the first naturally occurring ENaC antagonist to show improved preclinical efficacy in animal models of CF with no signs of renal toxicity.

INTRODUCTION

Cystic fibrosis (CF) is an autosomal recessive genetic disease caused by mutations in the cystic fibrosis transmembrane conductance regulator (*CFTR*) gene that results in absent or dysfunctional anion secretion across the apical membrane of epithelia (40). Although mutations in *CFTR* affect multiple organs, including the intestine, sweat glands, pancreas, and reproductive system, chronic lung disease is responsible for the vast majority of morbidity and mortality in CF patients (40, 53). In CF lungs, decreased transepithelial Cl^-/HCO_3^- secretion leads to acidification of the airway surface liquid (ASL) and hyperactivity of the epithelial Na^+ channel (ENaC). This, in turn, leads to excessive ASL absorption, the accumulation of dehydrated mucus, and an increased incidence of airway infections and inflammation (19, 45, 48, 53).

We have previously identified the secreted protein short palate lung and nasal epithelial clone 1 (SPLUNC1) as an endogenous inhibitor of ENaC and a modulator of ASL homeostasis (11). We have also identified the ENaC-inhibitory domain of SPLUNC1 and demonstrated that a naturally occurring 18-residue peptide (S18) derived from this region was able to inhibit ASL absorption for 24 h in human bronchial epithelial cells (HBECs) in a pH-independent manner (12, 18, 47). After resolving SPLUNC1's crystal structure, we demonstrated that SPLUNC1 exerted a pH-dependent inhibition of ENaC and, in the acidic environment of the CF airways, SPLUNC1 is unable to regulate ENaC as a result of two pH-sensitive salt bridges, which at acidic pH prevent SPLUNC1's ENaC-inhibitory domain from binding to ENaC (12). In contrast, S18 is pH independent in the absence of the salt bridges. Interestingly, while free S18 could be detected in normal sputum, this naturally occurring peptide was absent from CF sputum (18), suggesting that adding S18 back to CF airways may act as a replacement therapy.

Given the prominent role that Na^+ hyperabsorption plays in the pathophysiology of CF, aerosol delivery of an ENaC inhibitor offers an attractive therapeutic strategy to correct the underlying ASL abnormalities evident in CF airways (15). Early studies in this vein explored the use of amiloride and similar small molecule ENaC blockers. Unfortunately, given the low potency and easily reversible nature of these compounds, no evidence was found supporting their application in the treatment of CF respiratory conditions (8, 16, 17). These early studies also raised concerns over renal side effects, since

Address for reprint requests and other correspondence: R. Tarran, Marsico Lung Inst., The Univ. of North Carolina, Chapel Hill, NC 27599-7248 (e-mail: tarran@med.unc.edu).

amiloride and other related compounds are often readily absorbed across epithelial barriers allowing them to enter systemic circulation where they antagonize ENaC in the kidney, eliciting renal Na^+ loss and K^+ retention (2, 54). To be clinically efficacious, peptide therapeutics will need to be administered via inhalation and be able to freely diffuse through the thick, dehydrated CF mucus to reach the apical cell surface. They will also need to demonstrate an enhanced ability to restore lung hydration and improve mucus clearance without inducing a Na^+-wasting or K^+-sparing diuresis in the kidney. Given the hurdles that an inhaled peptide will need to overcome to reach its target, it is not known whether peptide-derived therapies will be efficacious for the treatment of CF lung disease. In this study, therefore, we utilized a variety of in vitro techniques and in vivo models of cystic fibrosis and renal physiology to interrogate the clinical potential of the naturally occurring S18 peptide for the treatment of CF lung disease.

METHODS

Experimental peptides and proteins. S18 (GGLPVPLDQTLPLNVNPA) and a positive control peptide for use in the quartz crystal microbalance with dissipation (QCM-D) assay (ARTKQTARKSTGGKAPRKQL-K-biotin) were synthesized and purified using automated 9-fluorenylmethyloxycarbonyl (Fmoc) solid phase peptide synthesis as previously described (9). The S18 peptide was either left with free termini or the NH_2-terminus was labeled with tetramethylrhodamine (TAMRA; S18-TAMRA) as indicated. SPLUNC1 protein was expressed and purified as previously described (12).

Tissue procurement and cell culture. Donor lungs were obtained using protocols approved by the University of North Carolina Committee on the Protection of the Rights of Human Subjects, and full written, informed consent was obtained from the subjects or their surrogates. Primary HBECs were grown from cells harvested by enzymatic digestion of human bronchial tissue, cultured on 12-mm Transwell permeable supports (Corning), and maintained at an air-liquid interface (ALI) for ~4 wk in University of North Carolina (UNC) ALI media as previously described (11). Human alveolar type 2 cells were isolated from donor lungs by enzymatic digestion as described and cultured for ~7 days on 6.5-mm Transwell clear inserts (Corning) in DMEM and 10% FBS with penicillin, streptomycin, gentamicin, and amphotericin (6). Primary murine tracheal epithelia were harvested by enzymatic digestion of excised tracheas from congenic C57BL/6N β-ENaC-transgenic (Tg) mice and wild-type littermates as previously described and cultured for up to 2 wk on 12-mm Transwell permeable supports (Corning; 33).

Antimicrobial and antibiofilm assays. Pseudomonas aeruginosa PAO1 (obtained from Dr. Matthew Wolfgang, University of North Carolina at Chapel Hill) were grown in Luria broth (LB) at 37°C for 24 h with shaking at 300 rpm. Colony-forming units (CFU) per milliliter were determined by serial dilution plating on LB agar plates. The antimicrobial activity of S18 was tested by incubating *P. aeruginosa* PAO1 in the presence of increasing concentrations (0–10 μM) of S18 or SPLUNC1 (control) as previously described (50). The bacterial cultures were grown overnight at 37°C and 300 rpm, and 10^6 CFU/ml were added to flat-bottom 96-well plates (Corning) with increasing doses of S18 or SPLUNC1. Plates were incubated at 37°C for 24 h. Bacterial growth was measured by serially diluting samples in Ringer solution and plating on LB agar plates to determine the number of CFU per milliliter. The antibiofilm activity of the S18 peptide was tested by incubating *P. aeruginosa* PAO1 as described above for 24 h at 37°C. Plates were washed at 24 h. Biofilms were fixed with methanol and stained with 1% crystal violet. After rinsing with distilled water, the stained biofilms were resolubilized with 33% acetic acid. Biofilm formation was measured at optical density 590 nm using a Sunrise plate reader (Tecan, Winooski, VT).

Fluorescence-based binding assays. For the standard binding assay, primary HBECs were washed mucosally with PBS, fresh media were added serosally, and where appropriate, dexamethasone was added 24 h before the experiment. On the day of experimentation, TAMRA-labeled S18 was added apically in 20 μl of modified Ringer solution (pH 6.0–7.5) and incubated for 1 h at 37°C. Cultures were then washed mucosally three times with 500 μl of 4°C PBS to remove unbound S18 and mucus, and serosal media were replaced with 4°C media. Cultures were then imaged using a Leica SP5 confocal microscope with a ×63 glycerol immersion objective. TAMRA fluorescence was acquired using a 561-nm laser, with emission collected at 575–625 nm.

For the competitive binding assay, SPLUNC1 protein was labeled with amine-reactive DyLight 488 (Thermo Fisher Scientific, Waltham, MA) per kit instructions. On the day of the experiment, S18 (100 μM) with a free NH_2 terminus was added apically in 20 μl of modified Ringer solution (pH 6.0–7.5) and incubated for 1 h at 37°C. Following S18 incubation, fluorescent SPLUNC1 (30 μM) was added mucosally to HBECs for an additional 1 h at 37°C. Cultures were then washed three times in PBS and imaged by epifluorescence microscopy as previously described (12) using a Nikon Ti-U microscope with a ×60 water immersion lens, Hamamatsu Orca camera, and Ludl filter wheels. For both assays, total fluorescence was quantified using ImageJ software (National Institutes of Health, https://imagej.nih.gov/ij/).

Superresolution microscopy. Mucus was collected from HBECs as described (22) and incubated overnight at 4°C with 25-nm fluorescent microspheres (Thermo Fisher Scientific), which bind to and label mucus (46). The sample was then incubated for an additional 6 h at 4°C with S18-TAMRA (10 μM), after which the sample was imaged using a Leica ground state depletion (GSD) superresolution microscope using a ×160 oil immersion objective to qualitatively assess colocalization.

Quartz crystal microbalance with dissipation assay. A semipurified, native mucus preparation that contained mucin 5B (MUC5B) and interacting proteins (39) was used for S18-mucus/mucin interactions. Briefly, semipurified MUC5B from the void of Sepharose CL-2B gel filtration chromatography was deposited on gold-coated quartz crystals for ~20 min as previously described (23, 39). Following the mucin deposition period, either S18 (1 mg/ml) or a positively charged control peptide designed to interact with mucus (ARTKQTARKSTGGKAPRKQL-K-biotin; 1 mg/ml) was introduced to the mucin layer, and changes in dissipation and frequency were monitored in real time. Once the system had again stabilized, a wash buffer (PBS) was added, and changes in dissipation and frequency were again monitored in real time. Qtools software (QSense; Biolin Scientific, Stockholm, Sweden) was then used to calculate layer viscosity, shear elasticity, and layer thickness.

Mucus penetration and diffusion assay. CF HBECs (ΔF508 homozygous) were cultured at an air-liquid interface for ~4 wk. Cultures were then prestained with 10-kDa Alexa Fluor 633-dextran (Thermo Fisher Scientific) and 25-nm FITC fluorescent microspheres (Thermo Fisher Scientific) to visualize the ASL and mucus, respectively. The cultures were then left unwashed for 8 days to accumulate a thickened mucus layer that was ~15% solids (46). Images of the ASL and mucus were then rapidly captured by *xz*-confocal microscopy using a Leica SP8 confocal microscope using a ×63 glycerol lens before and after the addition of S18-TAMRA. S18-TAMRA was added as a dry powder in perfluorocarbon FC-77 (3M, Maplewood, MN) as previously described (46).

ASL height measurements. ASL height studies were performed on alveolar type 2 cells, HBECs, and mouse epithelial tracheal cultures (MTECs) that had been washed for 30 min with 500 μl of PBS to remove the endogenous ASL. For the HBEC studies, normal HBECs were loaded with 20 μl of PBS containing S18 (100 μM), amiloride

hydrochloride (Sigma-Aldrich, St. Louis, MO; 100 μM), or nothing (vehicle), along with 100 nM human neutrophil elastase to maximally activate ENaC and 10-kDa tetramethylrhodamine dextran (Thermo Fisher Scientific) at 1 mg/ml to label the ASL. After 2 and 8 h of incubation at 37°C, ASL height was measured using a Leica SP5 confocal microscope with a ×63 glycerol immersion objective as previously described (52). For the MTEC studies, MTECs isolated from C57BL/6N β-ENaC-Tg mice or wild-type littermates were loaded with 20 μl of PBS containing 30 μM S18 or nothing (vehicle), along with 10-kDa tetramethylrhodamine dextran (Thermo Fisher Scientific) at 1 mg/ml. After a 4-h incubation at 37°C, the ASL height of the cultures was measured as described above. For alveolar type 2 cells, after washing the mucosal surface, 10 μl of PBS containing 100 μM S18, 100 μM amiloride, or nothing (vehicle), along with 10-kDa tetramethylrhodamine dextran (Thermo Fisher Scientific), were added mucosally, and height was measured by *xz*-confocal microscopy 2 h later. In all cases, perfluorocarbon (FC-77; 3M) was added apically during imaging to prevent ASL evaporation.

Electrophysiological measurements of relative ENaC currents. Electrophysiological studies were performed on normal HBECs that had been washed with 500 μl of PBS to remove the endogenous ASL. The cultures were then treated with 20 μl of PBS containing 100 nM neutrophil elastase (control) or 100 nM neutrophil elastase and 10 μM S18 for 1 h. Following 1 h, the cultures were washed again, and an additional 500 μl of PBS was added apically. Transepithelial electrical resistance (R_t) and voltage (V_t) were measured using an epithelial volt/ohmmeter (EVOM; World Precision Instruments, Sarasota, FL) in conjunction with a fixed pair of double electrodes positioned with one electrode in the serosal bath and the other in the apical compartment as previously described (44). To determine the amiloride-sensitive V_t, V_t was measured, amiloride (100 μM) was added serosally, and V_t was remeasured 10 min later with amiloride-sensitive V_t being the difference between these values. Equivalent currents were then calculated using Ohm's law ($V = I{\cdot}R$). Bumetanide (100 μM) was present serosally for all measurements to inhibit Cl^- secretion.

Mouse metabolic cage studies. Adult, male C57BL/6N mice were purchased from Charles River Laboratories in Raleigh, NC. Mice were housed in individually ventilated microisolator cages in a specific pathogen-free facility maintained at UNC Chapel Hill on a 12-h:12-h day-night cycle. All procedures were approved by the Institutional Animal Care and Use Committee of UNC Chapel Hill and performed according to the principles outlined by the National Institutes of Health guidelines for the care and use of animals in biomedical research. On the morning of experimentation, mice were given an intraperitoneal injection of 0.9% NaCl equal in volume to 10% body weight containing 100 μM S18, 100 μM amiloride hydrochloride (Sigma-Aldrich), or nothing (vehicle). Mice were then placed in individual metabolic cages (Techniplast, Milan, Italy) with preweighed urine collection tubes. Urine tubes were collected and replaced every 2 h for a total of 8 h. No food or water was provided during the 8-h urine collection study. Urine volume was measured gravimetrically, and urine Na^+ and K^+ levels were determined using a model 943 flame photometer (Instrumentation Laboratory, Lexington, MA).

Renal electrolyte and urine handling in anesthetized rats. Experiments were performed in 240–300-g male rats purchased from Charles River Laboratories. All procedures were approved by the Institutional Animal Care and Use Committee of UNC Chapel Hill and performed according to the principles outlined by the National Institutes of Health guidelines for the care and use of animals in biomedical research. On the day of experimentation, rats were anesthetized by intraperitoneal injection of 50 mg/kg pentobarbital sodium (Sigma-Aldrich) and placed on a SurgiSuite servo-controlled heating table (Kent Scientific, Torrington, CT) to maintain a body temperature of 37–38°C as measured by rectal probe. A tracheotomy tube [polyethylene (PE)-205] was inserted into the trachea to ensure a patent airway. The left carotid artery was cannulated (PE-50) for continuous recording of arterial pressure. Two catheters were inserted into the right jugular vein. The first jugular catheter (PE-50) was used for infusion of a maintenance solution consisting of 6% bovine serum albumin (BSA; Sigma-Aldrich) in 0.9% saline infused at 24 μl/min during the surgery and then reduced to 14 μl/min during the experimental periods. The second jugular catheter (PE-10) was used for infusion of FITC-inulin (Sigma-Aldrich) at 20 mg/ml and infused at 10 μl/min for determination of glomerular filtration rate (GFR). In all cases, the total infusion volume during the experimental periods was 24 μl/min. The abdomen was opened by a midline incision. The left renal artery was separated from the renal vein, and an ultrasonic flow probe (Transonic Systems, Ithaca, NY) was installed to measure renal blood flow (RBF). The ureters were individually cannulated (PE-10) for urine collection. Mean arterial pressure (MAP), heart rate, and RBF were continuously recorded by a four-channel PowerLab (AD-Instruments, Colorado Springs, CO). Upon completion of the surgical procedures, rats were allowed to stabilize for 60 min before the experimental protocol began.

The experimental protocol consisted of 6 × 30-min collection periods where urine was collected from the right and left kidneys to determine urine volume, urine flow rate, GFR, and urine electrolyte excretion. A carotid artery blood sample was taken at the midpoint of each period for the measurement of serum FITC-inulin concentration. The first 30-min collection period was used as a control period to determine baseline MAP, urine flow rate, RBF, urine electrolyte excretion, and GFR. For graphical purposes this 30-min control period is recorded as *time 0* (preinfusion). Infusion of S18 or amiloride hydrochloride (Sigma-Aldrich) commenced after this period and continued for the entirety of *period 2* (i.e., 0–30 min on graphs). At the time of drug infusion, the syringe supplying 6% BSA in 0.9% NaCl at 14 μl/min into the first jugular catheter was swapped with a syringe containing 6% BSA and amiloride in 0.9% NaCl or 6% BSA + S18 in 0.9% NaCl at a drug concentration adjusted to animal body weight to deliver 0.35 pmol·kg body $wt^{-1}{\cdot}min^{-1}$ for both drugs. Vehicle control animals received only the maintenance solution of 6% BSA in 0.9% NaCl during the infusion period. Urine volume was measured gravimetrically, and urine Na^+ and K^+ levels were determined using a model 943 flame photometer (Instrumentation Laboratory). Urine flow rate was normalized to kidney weight to account for variability in animal size. GFR was calculated as the clearance of FITC-labeled inulin, which was determined fluorometrically using Infinite M1000 plate reader (Tecan).

S18 treatment studies in neonatal β-ENaC-Tg mice. The generation and genotyping of β-ENaC-overexpressing (β-ENaC-Tg) mice on a congenic C57BL/6N background have been described previously (28, 32, 53). For the S18 treatment studies, hemizygous male C57BL/6N β-ENaC-Tg mice bred in house were crossed with female wild-type FVB/NJ mice (Charles River Laboratories) to produce FVB/NJ:C57BL/6N F1 β-ENaC-Tg pups. All animals were housed in individually ventilated microisolator cages in a specific pathogen-free facility maintained at UNC Chapel Hill on a 12-h:12-h day-night cycle. Breeding females were provided a high-energy breeder chow diet and given water ad libitum. All animal procedures were approved by the Institutional Animal Care and Use Committee of UNC Chapel Hill and performed according to the principles outlined by the National Institutes of Health guidelines for the care and use of animals in biomedical research. S18 or amiloride hydrochloride (Sigma-Aldrich) was dissolved in sterile distilled water (ddH_2O). After temporary anesthesia with 5% isoflurane (Baxter, Deerfield, IL) with 1 l/min O_2 using an isoflurane vaporizer (VetEquip, Livermore, CA), newborn FVB/NJ:C57BL/6N F1 β-ENaC-Tg pups were treated by intranasal instillation three times daily with S18 (100 mM at 1 μl/g body wt), amiloride (10 mM at 1 μl/g body wt), or vehicle (ddH_2O at 1 μl/g body wt) for a period of 14 days. During the treatment period, growth and survival were monitored. Deficits in body mass observed in amiloride-treated mice were replaced by subcutaneous injections of 0.9% NaCl as previously described (54).

S18 pharmacodynamic studies in mice. Mice were intranasally instilled with 100 mM S18 at 1 μl/g body wt. Blood samples were obtained from four mice at each time point. Approximately 0.5–1 ml of whole blood was obtained from each animal via cardiac puncture. Blood samples were collected into tubes with no anticoagulant, allowed to clot for 30 min, and centrifuged 10 min at 2,000 *g*, and the serum was analyzed using mass spectrometry.

Mass spectrometry analysis of S18 peptides. Measurements of S18 levels in murine serum samples were performed using filter-aided sample preparation followed by liquid chromatography-tandem mass spectrometry (LC-MS/MS) analysis. To collect the low-molecular weight range fractions and to remove proteins and other high-molecular weight serum components, samples were ultrafiltrated using Microcon-10 spin filters with a cutoff at 10 kDa (Millipore). Fifty-microliter starting volume mouse serum low-molecular weight ultrafiltrates were diluted with an equal volume of 2% acetonitrile and 2% trifluoroacetic acid. Low-molecular weight serum sample constituents were separated using a Dionex Ultimate 3000 RSLC Nano liquid chromatography system coupled to a Q Exactive mass spectrometer and nanospray source (Thermo Fisher Scientific). One microliter per sample was injected and loaded into a trap column (Acclaim PepMap, 2 cm × 75 μm ID, C18, 3 μm, 100 Å; Dionex) at 5 μl/min with aqueous solution containing 0.1% (vol/vol) trifluoroacetic acid and 2% acetonitrile. Analytes were separated using an analytical column (Acclaim PepMap RSLC, 15 cm × 75 μm ID, C18, 2 μm, 100 Å; Dionex) on a linear gradient of 4–30% *solvent B* (99.9% acetonitrile with 0.1% formic acid) over 60 min at a flow rate of 0.3 μl/min. Mass spectrometry analysis was performed using a method combining a targeted selected-ion monitoring (tSIM) scan with time-scheduled data-independent acquisition (DIA). In a tSIM event, data were acquired at a resolution of 70,000 at a mass-to-charge ratio (*m/z*) of 200, with a target automatic gain control (AGC) value of 5×10^5 and maximum fill times of 200 ms, a multiplex degree of 6, and an isolation width of 3 *m/z*. The subsequent DIA scan was triggered by a time-scheduled inclusion list with a ±5-min retention time window. The DIA scan was performed at a resolution of 35,000, isolation window of 3.0 *m/z*, target AGC values of 2×10^5, maximum fill times set to auto with equal individual fill times, and multiplex degree of 2. Fragmentation was performed with a normalized collision energy of 27. Raw data acquisition files obtained from the tSIM-DIA analyses of the mouse serum ultrafiltrate samples were processed using Skyline (version 3.6; 31). After identification of the S18 peptide peak using MS/MS, fragmentation information peak areas of the S18 precursor ion *m/z* 908.0042++ were calculated for each sample. The final S18 sample concentration was determined using a calibration curve using linear regression of the measured S18 standards between 1.6 and 100 fmol/μl (nM).

Reversal of CFTR inhibitor-induced reduction of tracheal mucus velocity assay. Experiments were conducted in adult ewes at Mount Sinai Medical Center under the approval of the Mount Sanai Medical Center Animal Research Committee. Tracheal mucus velocity (TMV) was measured by a roentgenographic technique in conscious sheep as previously described (17). Briefly, sheep were restrained upright in a specialized supportive cart. After topical anesthesia of the nasal passages with a 2% lidocaine solution, the sheep were nasally intubated with a 7.5-cm-inner diameter endotracheal tube (Mallinckrodt Medical, St. Louis, MO) and 5–10 radiopaque Teflon trioxide disks, ~1 mm in diameter, 0.8 mm thick, and 1.5–2 mg in weight, were introduced into the trachea via the endotracheal tube. The particles were insufflated by a modified suction catheter connected to a source of compressed air at a flow of 3–4 l/min at 50 lb./in.^{2}. The catheter remained within the endotracheal tube during insufflation to avoid contact with the tracheal surface and was removed following insufflation. To help minimize effects on TMV caused by endotracheal cuff inflation, the cuff was only inflated during the period of drug delivery. To prevent desiccation of the tracheal mucosa as a result of prolonged intubation, the inspired air was warmed and humidified using a Bennett humidifier (Puritan Bennett, Lenexa, KS). The disk movements were recorded using videotaped fluoroscopy, and the cephaladaxial velocities of the individual disks were calculated by measuring the distance traveled by each disk over a 1-min period. A collar containing radiopaque reference markers of known length was placed around the sheep's neck and used as a standard to correct for magnification effects intrinsic to the fluoroscopy unit. At each time point, the mean of all individual disk velocities was calculated.

A baseline TMV measure was initially obtained followed by aerosolization of CFTR inhibitor 172 [CFTR(inh)-172; 10 mg] dissolved in 0.3 ml DMSO and 2.7 ml ethanol. The total volume of CFTR(inh)-172 was delivered to each animal using an AirLife Misty Max 10 medication inhaler (CareFusion, San Diego, CA), and subsequent TMV measures were obtained every hour for a total of 12 h. Immediately following the 4-h TMV reading, nebulized aerosols of S18 (4 mg/kg), amiloride (0.06 mg/kg), or vehicle (0.9% NaCl, pH 7.0) were delivered directly into the trachea of the sheep using an AirLife Misty Max 10 medication inhaler. A dosimetry system activated by a piston respirator was used to deliver CFTR(inh)-172 or S18. Nebulized aerosols were delivered directly into the trachea only during an inspiration frequency of 20 breaths/min and at a tidal volume of 500 ml, as previously described (17).

Statistical analyses. Data were analyzed with GraphPad Prism 6.05 (GraphPad Software, La Jolla, CA). Unless otherwise noted, all data are presented as means ± SE for *n* experiments. Differences between means were tested for statistical significance using one-way analysis of variance (ANOVA), two-way ANOVA, Kaplan-Meier log-rank analysis, linear regression, and unpaired *t*-tests. From such comparisons, differences yielding values of $P < 0.05$ were judged to be significant.

RESULTS

S18 blocks the pH-dependent binding of SPLUNC1 to HBEC mucosal surfaces. We have previously identified the ENaC-inhibitory domain of SPLUNC1 and demonstrated that the naturally occurring S18 peptide, which corresponds to this region, binds to ENaC's β-subunit (18). Here, we show that HBECs pretreated with dexamethasone displayed increased ENaC protein levels (Fig. 1*A*) and an enhanced, dose-dependent ability to bind S18 (Fig. 1, *B* and *C*). We have also reported that SPLUNC1's ability to bind and regulate ENaC is pH dependent (12). We confirmed that fluorescently labeled SPLUNC1 binds to ENaC on the apical cell surface at pH 7.5, but not in the moderately acidic environment typical of the CF lung (pH 6.0; Fig. 1, *D* and *E*). We also show that pretreatment of the apical surface with S18 blocks the ability of fluorescently labeled SPLUNC1 to bind to ENaC at pH 7.5, suggesting that SPLUNC1 and S18 are binding to the same target (Fig. 1, *D* and *E*).

S18 does not interact with mucins and diffuses through dehydrated CF mucus. Mucus obstruction is a common presentation in the CF lung (38). In order for peptide therapeutics to be clinically efficacious, they will need to be freely diffusible in dehydrated CF mucus and not bind to mucins. We allowed CF HBECs, cultured at an air-liquid interface, to accumulate a thickened, dehydrated mucus layer that was ~15% solids by not washing their apical surface for 8 days (46). We prestained the ASL/mucus 24 h before experimentation with Alexa Fluor 647-dextran to label the ASL and 25-nm FITC beads to label mucus. S18-TAMRA was then added as a dry powder in perfluorocarbon to the apical surfaces, and images were rapidly captured by *xz*-confocal microscopy. S18-TAMRA was detectable at the cell surface within 30 s, sug-

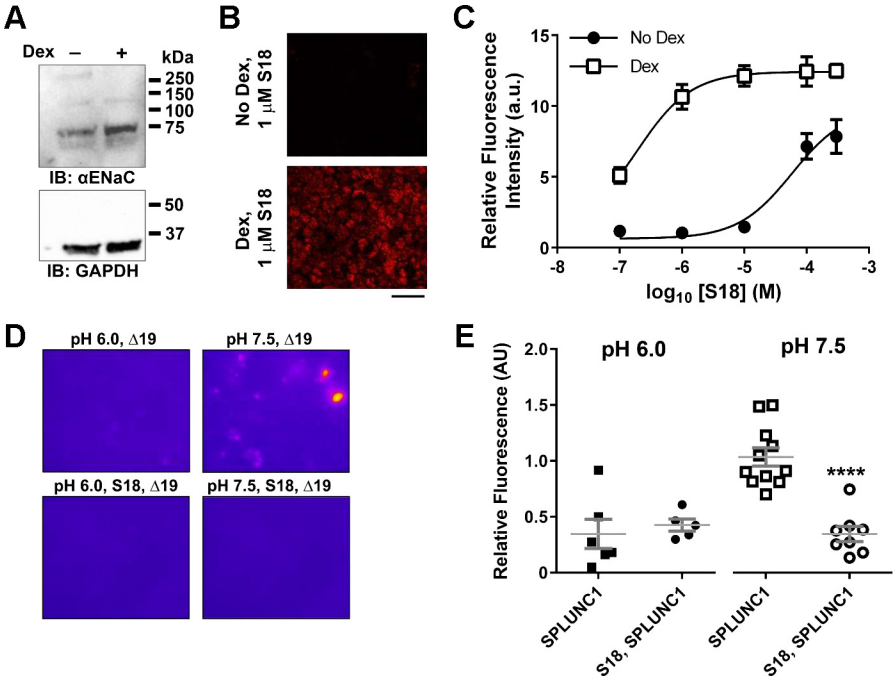

Fig. 1. S18 binds to human bronchial epithelial cell (HBEC) mucosal surfaces and blocks the pH-dependent binding of short palate lung and nasal epithelial clone 1 (SPLUNC1). *A*: representative Western blot showing epithelial Na^+ channel α-subunit (α-ENaC) expression in HBECs ± 24 h of 3 nM dexamethasone (Dex) treatment. IB, immunoblot. *B*: typical *xy*-confocal micrographs of tetramethylrhodamine (TAMRA)-labeled S18 (red) binding to the mucosal surface of HBECs in the presence and absence of 3 nM dexamethasone. *C*: dose response for TAMRA-tagged S18 binding to the mucosal surface of HBECs ± 24 h dexamethasone treatment, as measured by *xz*-confocal microscopy. All $n = 3$–5; a.u., arbitrary units. *D*: typical pseudocolored epifluorescent images of HBEC mucosal surfaces ± DyLight 488-SPLUNC1 either alone or following pretreatment with unlabeled S18. *E*: competitive binding of S18 and DyLight 488-SPLUNC1 to HBEC mucosal surfaces at pH 6.0 ($n = 5$) and pH 7.5 ($n = 8$–12). HBECs were either pretreated with S18 or vehicle for 1 h and then incubated with Alexa Fluor 488-labeled SPLUNC1 and imaged by epifluorescence microscopy. Squares, DyLight 488-SPLUNC1 alone; circles, S18 and then DyLight 488-SPLUNC1. Significance (****$P < 0.0001$) with respect to pH 7.5 cultures in the absence of S18 is indicated.

gesting that S18 is fully diffusible through dehydrated mucus layers (Fig. 2*A*). To directly assess S18's interactions with mucins, we incubated S18-rhodamine with HBEC-derived mucus and 10-nm fluorescent latex beads that bind to mucus (46) for 24 h and captured images by superresolution microscopy (~30-nm resolution). After 24 h of coincubation, there was no detectable colocalization between the mucus (i.e., the latex beads) and S18-TAMRA, further indicating that S18 does not interact with mucus (Fig. 2*B*).

To confirm and quantify these findings, S18-mucin interactions were measured by quartz crystal microbalance with dissipation (QCM-D). Under these conditions, S18 did not react with MUC5B and did not affect either frequency (indicative of protein binding) or dissipation (indicative of hydration/cross-linking; Fig. 2*C*). Using Voigt modeling (Qtools; Biolin Scientific), we calculated layer viscosity (1.07 ± 0.01 cP), shear elasticity (7,158 ± 220 Pa), and layer thickness (36.12 ± 0.09 nm) and found that none of these parameters were affected by the addition of S18 ($n = 4$). Since lysine-rich (polylysine) peptides have been shown to interact with mucins (23), we also tested the interaction between a positively charged control peptide (ARTKQTARKSTGGKAPRKQL-K-biotin) and MUC5B by QCM-D (Fig. 2*D*). As expected, the lysine-rich control peptide showed a sharp decrease in both frequency and dissipation (-52×10^{-6} to -64×10^{-6} and 10.6×10^{-6} to 8.5×10^{-6}, respectively) that remained following the wash step, suggesting substantial binding and cross-linking to the mucin layer. Using Voigt modeling, we found that the control peptide caused an increase in viscosity and shear elasticity, with a concurrent decrease in layer thickness (1.07 ± 0.05 to 1.19 ± 0.02 cP; 7,158 ± 205 to 10,259 ± 200 Pa; and 39.5 ± 0.05 to 25.5 ± 0.1 nm, respectively; $n = 4$). Taken together, these findings suggest that S18 does not interact with the main and most abundant molecule of the mucus gel, i.e., MUC5B.

S18 has neither antimicrobial nor antibiofilm activity against P. aeruginosa PAO1. SPLUNC1 has been previously reported to have antimicrobial activity (27, 42). Given that S18 is a SPLUNC1-derived peptide, we first assessed S18's potential antibiotic properties by incubating *P. aeruginosa* PAO1 with varying concentrations of S18 vs. full-length SPLUNC1, which served as a positive control. We then measured the number of colony-forming units (CFU) following standard plate-counting techniques. As previously described, SPLUNC1 caused a significant decrease in PAO1 CFU (Fig. 3*A*). We also cultured PAO1 in 96-well plates overnight to allow biofilm formation and measured optical density following crystal violet staining as a marker of biofilm density. SPLUNC1 significantly reduced PAO1 biofilm formation (Fig. 3*B*). In contrast, S18 did not display any antimicrobial or antibiofilm activity (Fig. 3, *A* and *B*).

S18 is more efficacious at reducing ASL absorption than amiloride. We also directly tested the ability of S18 to slow ASL absorption compared with amiloride under thin film conditions (Fig. 4). For this, we loaded normal HBECs with a 20-μl bolus of PBS containing 100 nM neutrophil elastase (to maximally activate ENaC), dextran (to label the ASL), and 100 μM of the appropriate test solution. We then used *xz*-confocal microscopy to track ASL absorption over 8 h. S18 addition resulted in a significantly greater increase in ASL height at both 2 and 8 h compared with vehicle treatment. In contrast, we found that amiloride treatment showed no ability to delay ASL absorption at either time point (Fig. 4, *A* and *B*). To verify that our HBECs exhibited amiloride sensitivity, we measured their bioelectric properties. Interestingly, under thick film conditions, where 500 μl of PBS were applied to culture surfaces, amiloride was capable of reducing both voltage and current (Fig. 4, *C* and *D*, respectively). Under these conditions, S18 pretreatment significantly reduced the amiloride sensitivity, suggesting

that S18 and amiloride both bind to the same target, i.e., ENaC. Since ENaC is also expressed in the alveolar regions of the lung (34), we also tested whether S18 could inhibit ENaC in cultured human alveolar type 2 cells. When added at equimolar concentrations (i.e., 100 μM), S18 but not amiloride prevented ASL absorption across these cultures (Fig. 4, *E* and *F*).

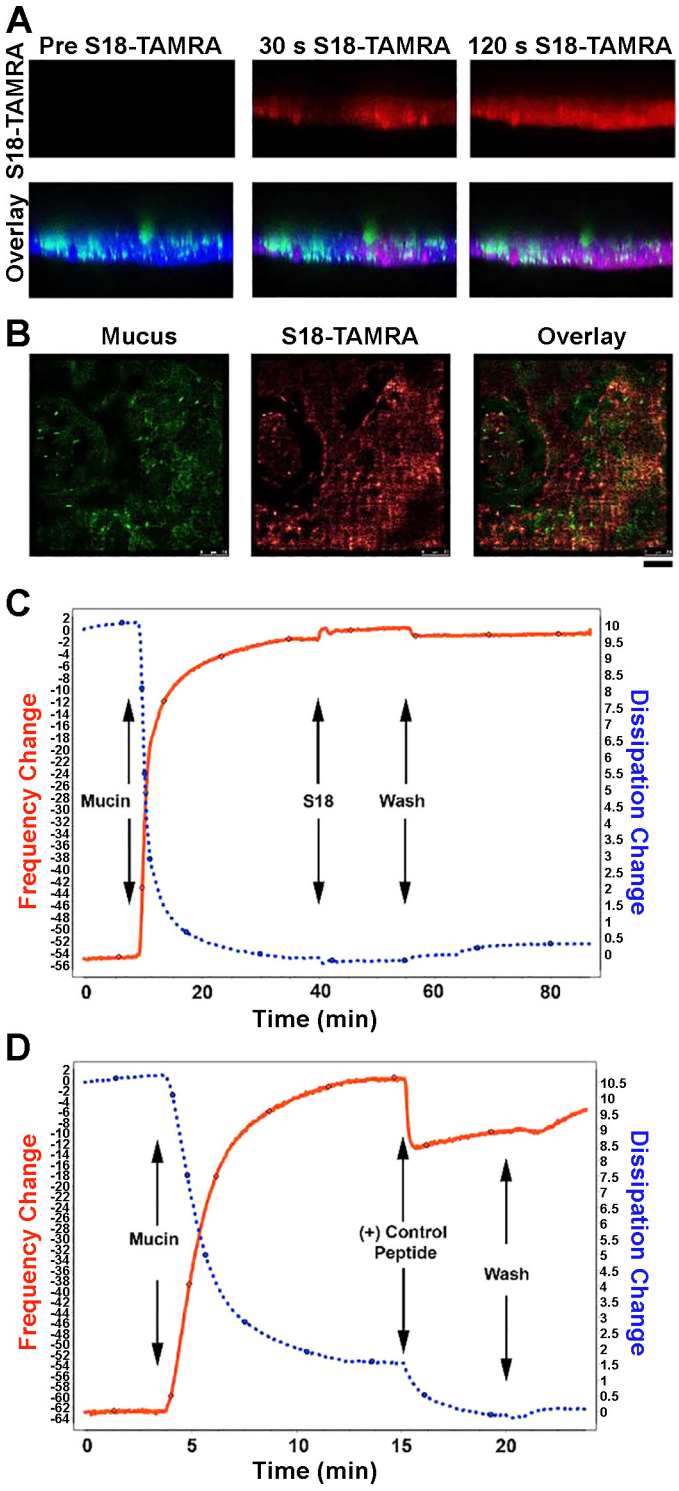

S18 does not induce sodium-wasting or potassium-sparing diuresis. Prior attempts to treat CF lung disease by inhalation of ENaC inhibitors have resulted in natriuresis/diuresis and subsequent hyperkalemia due to off-target effects on ENaC in the kidneys (2, 36, 54). To investigate the effects of S18 on renal homeostasis, we first looked for effects in conscious mice housed in metabolic cages. For this, we volume loaded wild-type C57BL/6N mice with intraperitoneal injections of 10% body weight isotonic saline containing S18 (100 μM), amiloride (100 μM), or vehicle (0.9% NaCl). Mice were then placed in metabolic cages, and urine was collected every 2 h to determine urine volume and Na^+ and K^+ output over 8 h. Following this protocol, we observed no detectable differences between S18- and vehicle-treated animals. In amiloride-treated animals, however, at 4-h posttreatment we observed a significant diuresis (41.4% increase in urine volume), natriuresis (64.2% increase in urinary Na^+), and antikaliuresis (66.4% decrease in urinary K^+) compared with vehicle-treated animals that persisted for the remainder of the study (Fig. 5, *A–C*).

To further confirm the lack of renal side effects with S18, we directly monitored renal function and blood pressure in real time in sedated rats. Here, blood pressure, heart rate, and renal blood flow were directly monitored by telemetry. Furthermore, glomerular filtration rate was monitored by infusing FITC-inulin into the carotid jugular and measuring its secretion by the kidneys, and blood and urine were collected at timed intervals to measure electrolytes. Anesthetized rats were given 30-min infusions of amiloride or S18 estimated to give serum drug concentrations of ~100 μM. Amiloride (0.35 pmol·kg body wt^{-1}·min^{-1}), S18 (0.35 pmol·kg body wt^{-1}·min^{-1}), or vehicle (6% BSA in 0.9% NaCl) were directly infused into their bloodstream. Following this protocol, mean arterial pressure, glomerular filtration rate, and renal blood flow were relatively stable throughout the experiments and did not differ between the groups (see Table 1). We also observed no detectable differences in urine flow between S18- and vehicle-treated animals (Fig. 6*A*). In contrast, amiloride infusion resulted in a rapid 180% increase in urine flow that peaked 30 min after the infusion was completed. Following this point, urine flow remained significantly elevated (~150% compared with vehicle-infused animals) for one additional period, after which no detectable differences in urine flow were observed between treatment groups (Fig. 6*A*).

To observe changes in ion excretion that were independent of urine volume, fractional and total ion excretion of Na^+ and K^+, along with serum K^+ levels, were determined in all groups

Fig. 2. S18 peptide does not interact with mucus. *A*: cystic fibrosis human bronchial epithelial cells (homozygous ΔF508) were left undisturbed for 8 days to generate a dehydrated, mucus-rich airway surface liquid (ASL) and were then stained with 10-kDa Alexa Fluor 633-dextran (ASL, blue) and 25-nm FITC microspheres (mucus, green) 24 h before experimentation. Images of ASL and mucus were captured by *xz*-confocal microscopy before and after addition of S18-tetramethylrhodamine (S18-TAMRA; red) added mucosally as a dry powder in perfluorocarbon at $t = 0$. Scale bar = 10 μm; $n = 3$. *B*: superresolution microscopy images of S18-TAMRA (red) and 10-nm FITC microspheres that bind to mucus (green). Resolution is 30 nm^2/pixel; scale bar = 2.5 μm. Images are representative of three separate experiments. *C* and *D*: quartz crystal microbalance with dissipation was used to quantify S18-mucus/mucin interaction by measuring the frequency shift (F7, blue) and dissipation shift (D7, red) of S18 ($n = 4$; *C*) or a lysine-rich control peptide ($n = 4$; *D*) binding to a semipurified, native mucus preparation.

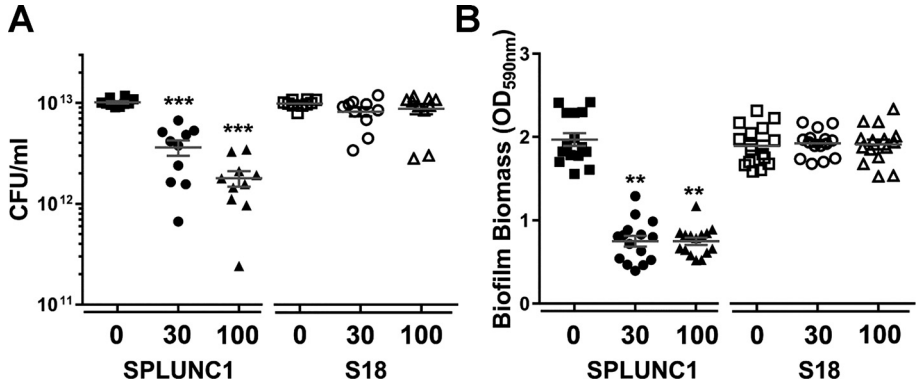

Fig. 3. S18 does not have antimicrobial or antibiofilm activity against *P. aeruginosa* PAO1. Increasing concentrations of short palate lung and nasal epithelial clone 1 (SPLUNC1) and S18 peptide were incubated with 10^6 colony-forming units (CFU)/ml *P. aeruginosa* strain PAO1 for 24 h, and subsequent bacterial growth and biofilm biomass were measured, respectively. *A*: SPLUNC1 but not S18 reduced bacterial growth (CFU counts). All $n = 10$. *B*: SPLUNC1 but not S18 reduced bacterial biofilm biomass, as indicated by 1% crystal violet staining and measurements at optical density 590 nm ($OD_{590\ nm}$). All $n = 15$. Data are shown as means ± SE. Significance (**$P < 0.01$, ***$P < 0.001$) with respect to vehicle-treated cultures is indicated.

throughout the experimental protocol. Similar to urine flow, we observed no detectable differences in fractional Na^+ or K^+ excretion between S18- and vehicle-treated animals (Fig. 6*B*). Amiloride infusion, however, resulted in an immediate increase in Na^+ excretion and an immediate decrease in K^+ excretion. The maximal change in Na^+ excretion occurred 1 h after the amiloride infusion (Fig. 6*B*). As predicted by inhibition of ENaC in the kidneys, amiloride infusion resulted in a nearly complete shutdown of K^+ excretion, which remained depressed throughout the remainder of the experiment (Fig. 6*C*). We also measured the serum K^+ concentrations throughout the study and found no difference between S18- and vehicle-infused animals. In contrast, we found that the amiloride-induced decrease in urinary K^+ excretion (Fig. 6*C*) was accompanied by a significant increase in serum K^+ levels compared with vehicle-infused animals (Fig. 6*D*).

Preventive S18 therapy reduces mortality and improves growth in β-ENaC-Tg mice. After demonstrating that S18 was able to improve ASL hydration (Fig. 4), we next evaluated the therapeutic efficacy of preventive S18 treatment using the β-ENaC-overexpressing (β-ENaC-Tg) mouse model of CF lung disease (32). We first confirmed that S18 was functional in murine tracheal epithelia by measuring the effect of S18 on ASL height in both wild-type and β-ENaC-Tg tracheal epithelial cultures. In line with previous reports (32), overexpression of β-ENaC resulted in an ~58% reduction of ASL height compared with wild-type MTECs (Fig. 7, *A* and *B*). At 4 h posttreatment, S18 improved ASL height of wild-type cultures by ~102% and of β-ENaC-Tg cultures by 320% compared with vehicle, suggesting that the β-ENaC mouse was a valid model to study the effect of S18.

Newborn mice are obligate nose breathers. Zhou et al. have demonstrated that 10 mM amiloride added intranasally prevents the development of lung disease in β-ENaC pups if administered every day after birth by inhibiting ENaC and preventing ASL dehydration (54). Using this regimen, they estimated that ~1% of the drug reaches the small airways. Accordingly, we treated newborn β-ENaC-Tg pups from the first day of life with amiloride (10 mM; 1 μl/g body wt), S18 (100 mM; 1 μl/g body wt), or vehicle (ddH_2O; 1 μl/g body wt) three times daily by intranasal instillation and monitored *postnatal day* (PND) *14* mortality and growth. Compared with preventive treatment with vehicle, which had 86.7% mortality at PND 14, amiloride treatment showed no reduction in mortality (88.9% at PND 14; Fig. 7*C*). In contrast, treatment with S18 resulted in an overall reduction in pulmonary mortality by ~46% (46.7% mortality at PND 14; Fig. 7*C*). Using linear regression analysis of the calculated slopes, we also compared the growth in body mass of the mice over the 14-day treatment period. When compared with vehicle treatment (slope = 36.0 ± 0.6, $r^2 = 0.97$), amiloride treatment resulted in an immediate and substantial loss of body mass (slope = 16.4 ± 0.3, $r^2 = 0.97$), whereas treatment with S18 resulted in a modest, but significant, improvement in body mass (slope = 40.3 ± 0.6, $r^2 = 0.96$; Fig. 7*D*). To better understand S18's pharmacodynamics, we then added 100 mM S18 intranasally and obtained blood by cardiac puncture. With the use of mass spectrometry, human S18 standards could be readily identified in murine blood (Fig. 7*E*) and were present at ~1 nM after addition, suggesting that only a very small fraction of inhaled S18 peptide reaches the bloodstream (Fig. 7*F*).

S18 reverses CFTR(inh)-172-induced reduction of tracheal mucus velocity in sheep. CFTR(inh)-172 is an allosteric inhibitor of CFTR that has previously been shown to reduce airway surface liquid height (30, 45). Aerosolization of 10 mg of CFTR(inh)-172 resulted in a slowing of TMV to ~54% of baseline after 2 h (Fig. 8), suggesting that CFTR(inh)-172-challenged sheep can act as a surrogate for early CF lung disease. We next evaluated the ability of S18 to restore normal mucus transport in sheep challenged with CFTR(inh)-172. Immediately following the 4-h TMV reading, either S18 (4 mg/kg), amiloride (0.06 mg/kg), or vehicle (0.9% NaCl) was aerosolized directly into the trachea using an AirLife medication nebulizer. Aerosolization of normal saline did not increase TMV, whereas an equal volume of S18 resulted in a near-complete reversal of CFTR(inh)-172-induced reduction of TMV by 1 h posttreatment (93 ± 3.6% of baseline) that persisted for the remainder of the observation period (i.e., 8 h; Fig. 8). Consistent with clinical observations (14, 24), amiloride transiently improved TMV but, unlike S18, failed to maintain improved mucus transport for extended periods.

DISCUSSION

Much evidence supports the hypothesis that the pathophysiology of CF lung disease is caused by reduced anion secretion and elevated cation absorption, which lead to ASL volume depletion and reduced mucociliary clearance (5, 10, 32, 35, 38, 46). Given that S18 but not SPLUNC1 can regulate ENaC/ASL volume in CF HBECs, that SPLUNC1 is cleaved by neutrophil elastase, and that endogenous, naturally occurring S18 is ab-

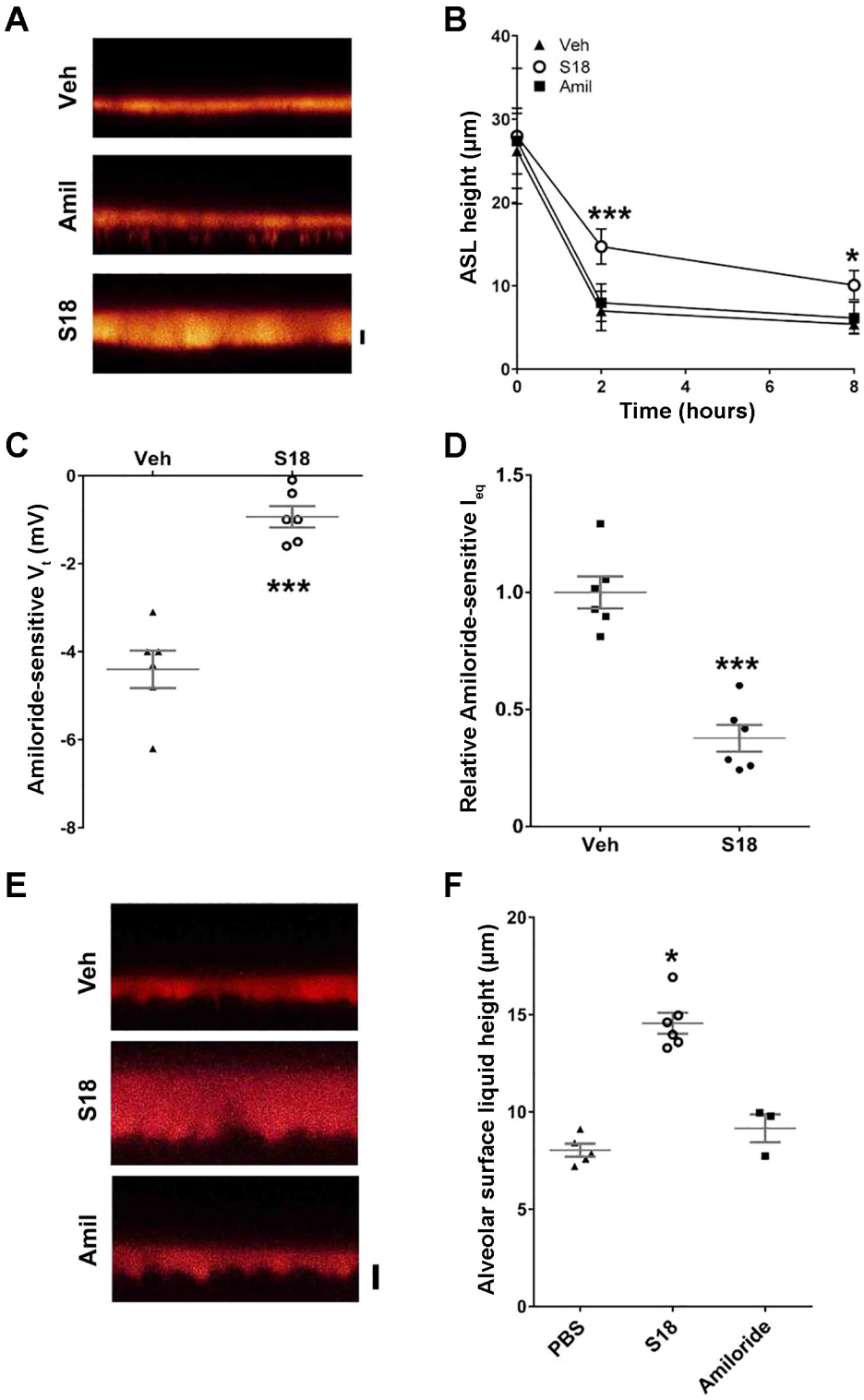

Fig. 4. S18 but not amiloride slows airway surface liquid (ASL) absorption under thin film conditions in human bronchial epithelial cells (HBECs) and alveolar type 2 cells. *A*: at $t = 0$, normal HBECs were loaded with 20 μl of PBS containing 1 mg/ml 10-kDa rhodamine dextran and 100 nM hydroxynonenal to maximally activate ENaC. Where indicated, S18 or amiloride (Amil) was added. Representative *xz*-confocal micrographs of ASL height (red) 8 h after addition of test compounds are shown. Veh, vehicle. *B*: plot of mean ASL heights over time. S18 (○, 100 μM, $n = 9$), amiloride (■, 100 μM, $n = 3$), or vehicle (▲, PBS alone, $n = 8$). *C* and *D*: mean amiloride-sensitive transepithelial voltage V_t and equivalent current I_{eq}, respectively, after vehicle (PBS) and vehicle plus 10 μM S18. Both $n = 6$. *E*: alveolar type 2 cell cultures were loaded with 10 μl PBS containing 1 mg/ml 10-kDa rhodamine dextran and 100 μM of amiloride or S18 where indicated. Representative *xz*-confocal micrographs of alveolar surface liquid height (red) 2 h after addition of test compounds are shown. *F*: mean alveolar surface liquid height taken 2 h after addition of vehicle or compound. Vehicle, $n = 5$; S18, $n = 6$; amiloride, $n = 3$. Significance ($^*P < 0.05$, $^{***}P < 0.001$) compared with vehicle is indicated.

sent from the bronchoalveolar lavage fluid of CF patients (12, 18, 20), our rationale is that inhaled peptide replacement therapy may serve to rebalance ASL and improve mucus hydration in CF patients. We have already studied S18-ENaC interactions in vitro (18). With a view to moving peptide therapeutics into the clinic for the treatment of CF, we tested the hypothesis that S18 can be efficacious in vivo without causing off-target renal effects. We first demonstrated that HBECs pretreated with dexamethasone displayed increased ENaC levels and an enhanced, dose-dependent ability to bind S18 (Fig. 1, *A–C*), suggesting that S18 binds to ENaC. We also showed that pretreatment of the apical surface with S18 blocks SPLUNC1 binding, suggesting that they bind the same target, i.e., ENaC (Fig. 1, *D* and *E*).

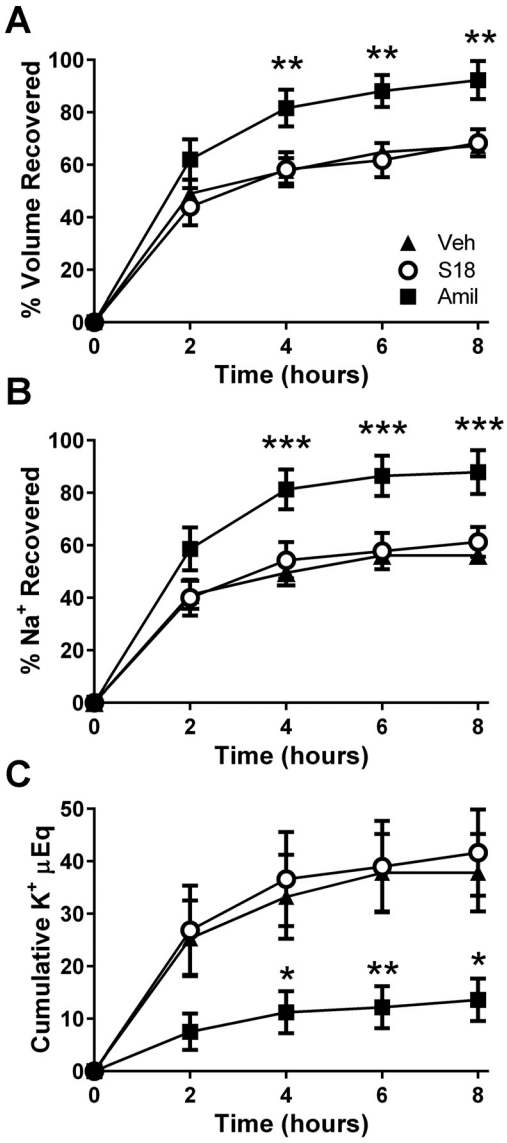

Fig. 5. Acute administration of S18 in conscious mice does not induce a sodium-wasting or potassium-sparing diuresis. Adult C57BL/6J wild-type male mice were injected intraperitoneally with a 0.9% NaCl bolus equal to 10% of body weight containing S18 (○, 100 μM, $n = 10$), amiloride (Amil, ■, 100 μM, $n = 10$), or vehicle (Veh, ▲, 0.9% NaCl alone, $n = 10$). Mice were then placed in metabolic cages, and urine was collected every 2 h for 8 h. *A*: urine volume output expressed as a cumulative percentage of the administered volume load plotted against collection time. *B*: urine Na^+ output expressed as a cumulative percentage of administered Na^+ in the loading volume plotted against collection time. *C*: cumulative urine K^+ output. Significance (*$P < 0.05$, **$P < 0.01$, ***$P < 0.001$) with respect to vehicle-treated mice is indicated.

CF lungs are characterized by a thickened mucus layer and mucus plugging (38). Since S18 is a peptide, we were concerned that it might become trapped in this thickened mucus layer and thus be unable to regulate ENaC at the apical cell surface. Through a series of cell-free experiments using QCM-D, confocal microscopy, and superresolution microscopy, we demonstrated that S18 does not interact with human mucus (Fig. 2, *A–D*). We also confirmed that S18 was rapidly able to penetrate CF mucus to reach the apical cell surface (Fig. 2*A*). Note that here S18 was added as a dry powder, which constitutes a "worst-case scenario" since the S18 will need to dissolve before it can diffuse. These findings are supported by our present understanding of CF mucus, which predicts that individual strands of gel-forming mucins create a mucin "mesh" and that the pores of this mesh are too large to trap S18 based on size alone. That is, the predicted pore size of a CF mucin mesh is ~200 nm, while S18 is ~1 nm (assuming that it is linear), so penetration is not predicted to be a major issue (26). Indeed, our superresolution data, which yield a resolution of ~30 nm^2/pixel, indicated that S18-TAMRA and mucin-bound 10-nm FITC beads did not colocalize (Fig. 2*B*), suggesting that S18 can indeed move in the spaces within the mucin mesh. Additionally, since S18 is a lysine-free peptide, we would not expect significant peptide-mucin interactions. These observations were reiterated by QCM-D, and here we demonstrated that a lysine-rich control peptide bound to MUC5B, while S18 did not (Fig. 2, *C* and *D*).

In addition to regulating ENaC, SPLUNC1 also exerts antimicrobial effects against gram-negative bacteria (7, 50). Consistent with these data, full-length, recombinant SPLUNC1 exerted antimicrobial and antibiofilm properties against *P. aeruginosa* PAO1 (Fig. 3, *A* and *B*). Our recent data suggested that SPLUNC1's antimicrobial activities were attributed to SPLUNC1's α4- and α6-helixes (1). However, at similar concentrations, S18 had no effect on *P. aeruginosa* growth or biofilm formation (Fig. 3), suggesting that chronic addition of S18 would not induce antimicrobial resistance in CF patients.

Early attempts to inhibit ENaC to treat CF lung disease utilized aerosol delivery of amiloride, an orally active, potassium-sparing diuretic (17). In 2006, Burrows et al. (8) published a comprehensive review of these trials and found no evidence of improvement in lung function in people with CF following amiloride treatment. Despite being able to inhibit

Table 1. *Mean arterial pressure and renal function data for amiloride-, S18-, and vehicle-infused rats*

Treatment and Time	n	MAP, mmHg	GFR, μl·min^{-1}·g kidney wt^{-1}	RBF, ml/min
Vehicle	7			
0 min		113.1 ± 1.7	2606.4 ± 300.3	6.7 ± 0.3
30 min		111.3 ± 2.7	2408.9 ± 267.2	6.8 ± 0.4
60 min		110.4 ± 3.1	2454.5 ± 294.1	6.9 ± 0.4
90 min		110.1 ± 2.9	2377.2 ± 201.8	7.0 ± 0.4
120 min		110.9 ± 3.2	2314.5 ± 236.0	6.9 ± 0.5
150 min		110.6 ± 3.2	2283.7 ± 233.3	6.8 ± 0.4
Amiloride	7			
0 min		115.8 ± 3.9	2709.0 ± 494.7	6.9 ± 0.8
30 min		115.2 ± 3.3	2591.2 ± 439.2	7.2 ± 0.8
60 min		113.3 ± 2.6	2164.6 ± 474.3	7.3 ± 1.0
90 min		117.1 ± 2.1	1938.2 ± 523.1	7.4 ± 1.0
120 min		116.6 ± 2.6	2002.0 ± 762.8	6.9 ± 0.9
150 min		114.7 ± 4.7	1718.7 ± 512.8	6.6 ± 0.8
S18	7			
0 min		112.7 ± 2.9	2787.3 ± 672.1	6.1 ± 0.4
30 min		113.3 ± 2.8	2649.4 ± 430.2	6.4 ± 0.5
60 min		113.4 ± 5.3	2816.8 ± 505.1	6.4 ± 0.5
90 min		113.6 ± 5.3	2722.4 ± 480.6	6.8 ± 0.7
120 min		114.1 ± 4.6	2990.8 ± 568.5	6.9 ± 0.7
150 min		115.0 ± 4.6	2667.3 ± 517.1	6.7 ± 0.7

Values are means ± SE; n = number of animals per group. Time 0 min = preinfusion control values. Amiloride (0.35 pmol·kg body wt^{-1}·min^{-1}), S18 (0.35 pmol·kg body wt^{-1}·min^{-1}), or vehicle (6% BSA in 0.9% NaCl) was infused from 0 to 30 min. MAP, mean arterial pressure; GFR, normalized glomerular filtration rate; RBF, renal blood flow.

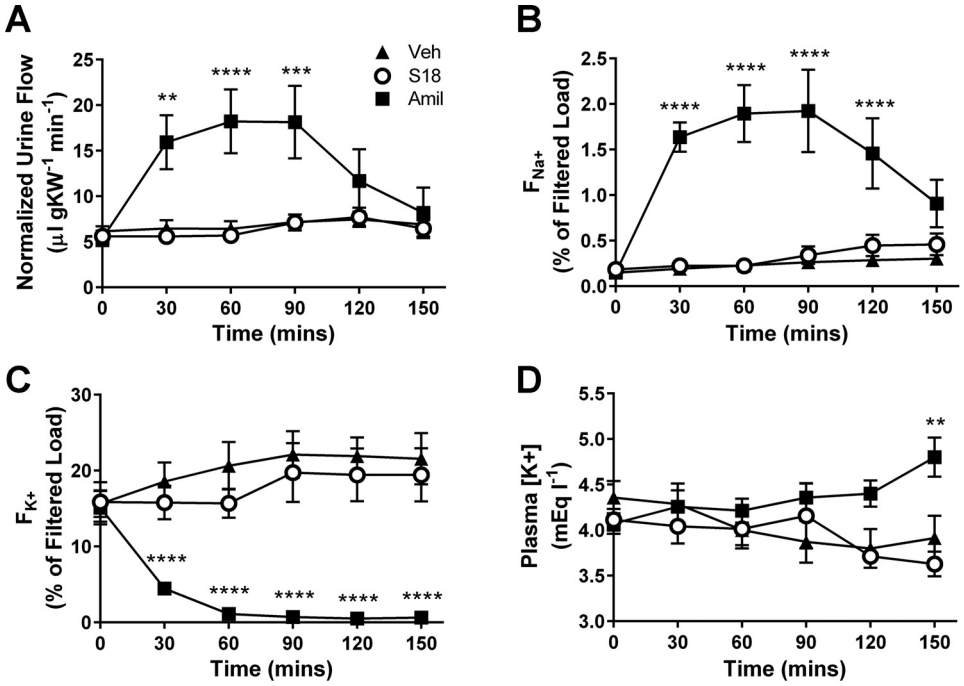

Fig. 6. Acute administration of S18 in anesthetized rats does not induce a Na^+-wasting or K^+-sparing diuresis. Adult male Sprague-Dawley rats were surgically fitted for urine and serum analysis. After collecting a 30-min baseline period ($t = 0$), rats were infused with amiloride (Amil, ■, 0.35 pmol·kg body wt^{-1}·min^{-1}, $n = 7$), S18 (○, 0.35 pmol·kg body wt^{-1}·min^{-1}, $n = 7$), or vehicle (Veh, ▲, 6% BSA in 0.9% NaCl, $n = 7$), and urine and serum were collected every 30 min for a subsequent 2.5 h. *A*: urine output during 30-min collection periods, expressed as a rate of µl·min^{-1}·g kidney wt $(gKW)^{-1}$. *B*: fractional Na^+ (F_{Na+}) excretion during 30-min collection periods, expressed as a percentage of filtered load. *C*: fractional K^+ excretion during 30-min collection periods, expressed as a percentage of filtered load. *D*: serum K^+ concentration, expressed as meq/l. Significance (**$P < 0.01$, ***$P < 0.001$, ****$P < 0.0001$) with respect to vehicle-treated rats is indicated.

Na^+ absorption at submicromolar concentrations in Ussing chambers, amiloride likely failed because it is readily absorbed across the airway and excreted by the kidneys. Indeed, it has been demonstrated that it has a very short half-life in the lung lumen (16, 17, 25, 46), which likely explains why we observed little effect of amiloride on ASL height (Fig. 4, *A, B, E,* and *F*), despite seeing significant effects of amiloride on V_t and equivalent current I_{eq} (Fig. 4, *C* and *D*). We have previously

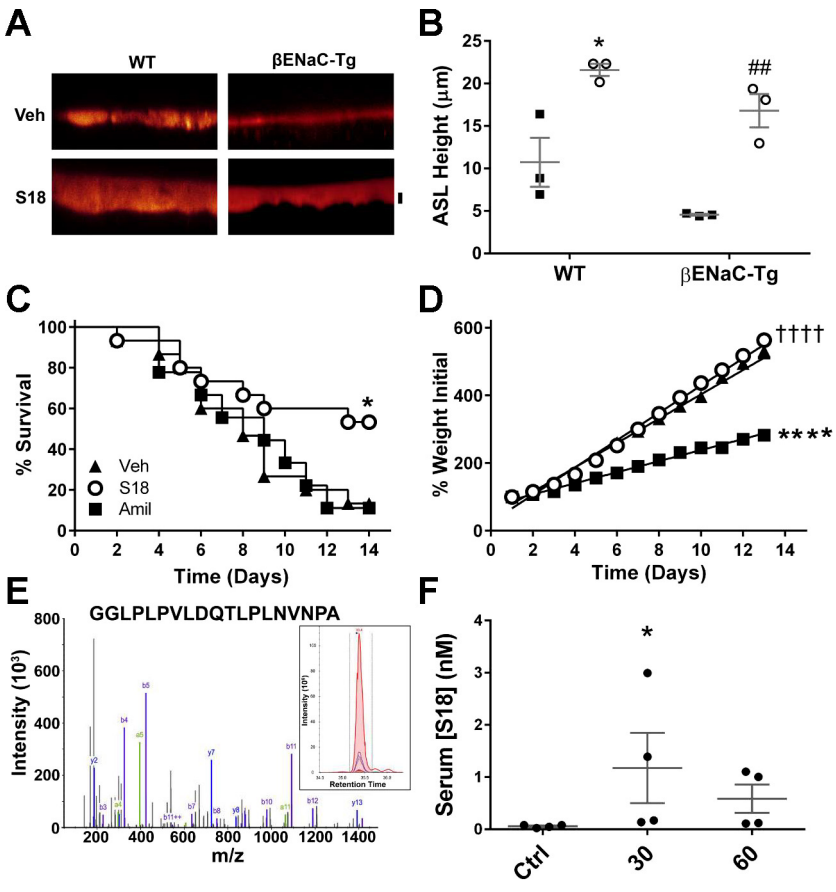

Fig. 7. Preventive treatment with S18 reduces mortality and improves growth of neonatal epithelial Na^+ channel β-subunit (β-ENaC)-overexpressing (β-ENaC-Tg) mice. *A*: representative *xz*-confocal micrographs of airway surface liquid (ASL) height (red) 4 h after addition of 20 µl of PBS containing 1 mg/ml 10-kDa rhodamine dextran with S18 or vehicle (Veh) to wild-type (WT) and β-ENaC-Tg murine tracheal epithelial cultures. Scale bar = 7 µm. *B*: summary of ASL height measurements (all $n = 3$; ■, vehicle; ○, 100 µM S18). *C*: Kaplan-Meier survival curves for β-ENaC-Tg mice treated three times daily by intranasal instillation with S18 (100 mM, $n = 15$), amiloride (Amil, 10 mM, $n = 9$), or vehicle (ddH_2O, $n = 15$) for a period of 2 wk starting on the first day of life. *D*: weight gain during the 2-wk treatment period was fit using linear regression analysis, and the calculated slopes ($\Delta y/\Delta x$) were compared using one-way ANOVA. *E*: S18 was identified by liquid chromatography-tandem mass spectrometry (LC-MS/MS), and S18 was quantified over time in murine serum (*inset*). *m/z*, mass-to-charge ratio. *F*: mean serum S18 concentrations as measured by mass spectrometry (LC-MS/MS) over time. Ctrl, control; $n = 8$ samples from 4 mice per time point. Significance: *$P < 0.05$ with respect to vehicle-treated cultures from wild-type mice or compared with $t = 0$, ##$P < 0.01$ with respect to vehicle-treated cultures from β-ENaC-Tg mice, ††††$P < 0.0001$ with respect to amiloride-treated β-ENaC-Tg mice, ****$P < 0.0001$ with respect to vehicle-treated β-ENaC-Tg mice.

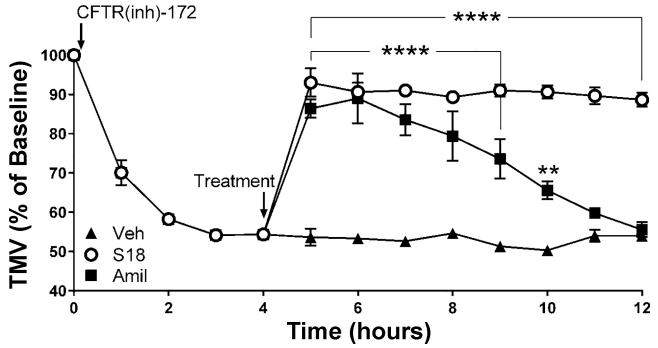

Fig. 8. S18 reverses cystic fibrosis transmembrane conductance regulator inhibitor 172 [CFTR(inh)-172]-induced reduction of tracheal mucus velocity (TMV). Immediately following a baseline TMV reading ($t = 0$), sheep were challenged with CFTR(inh)-172 (10 mg). Four hours later, S18 (○, 4 mg/kg, $n = 3$), amiloride (Amil, ■, 0.06 mg/kg, $n = 5$), or vehicle (Veh, ▲, 0.9% NaCl, $n = 3$) was delivered via nebulization. Significance (**$P < 0.01$, ****$P < 0.0001$) with respect to vehicle-treated sheep is indicated.

demonstrated that S18 can inhibit ASL absorption in CF HBECs for ≥24 h under thin film (i.e., nonflooded) conditions, suggesting that S18 stays in the ASL (18). Here, S18, but not amiloride, prevented ASL absorption over time (Fig. 4, *A* and *B*). This difference is likely the result of S18 being retained in the ASL for longer than amiloride but might also stem from differing mechanisms of action between S18 and amiloride. Unlike amiloride, which blocks ENaC's pore, S18 inhibits Na^+ absorption reducing ENaC surface densities (41), which likely reduces the reversibility of S18's inhibition and improves its duration of action.

The chronic inhibition of ENaC is likely safe for human subjects. In addition to our in vivo studies, the proof of concept for this approach comes in part from patients with type 1 pseudohypoaldosteronism (PHA1), who, through loss-of-function mutations in ENaC, absorb no Na^+ across tissues where ENaC predominates. As a result, PHA1 patients have increased ASL volume and higher rates of mucociliary transport compared with people with functional ENaC but do not suffer from respiratory dysfunction (21). Respiratory bronchioles and the alveolar surfaces play an important role in gas exchange, and since O_2 is poorly soluble in aqueous solutions, O_2 transport across the lung can be impaired during edema. However, we have previously measured the partial pressure of O_2 (P_{O_2}) in the ASL as a function of ASL height and found that at heights <50 μm, there was no change in P_{O_2} at the cell surface (51). SPLUNC1 and S18 are physiological regulators of ENaC that are naturally occurring in sputum/bronchoalveolar lavage fluid and can come into contact with ENaC throughout the lung, including at alveolar surfaces. Therefore, on the basis of the data shown in Fig. 4, *E* and *F*, and our published data (51), a functional doubling of alveolar height to ~15 μm would not affect O_2 transport.

Prolonged ENaC antagonism in the lung with small molecule inhibitors increases the incidence of renal side effects. For example, both amiloride and GS-9411, a high-potency ENaC antagonist, cause hyperkalemia (36, 54). Hyperkalemia was also observed with an ENaC antagonist generated by AstraZeneca in two different species (3). These side effects occur when small molecule ENaC antagonists are absorbed into the blood and are then freely filtered at the glomerulus to antagonize ENaC in the distal nephron, which results in a K^+-sparing natriuresis and diuresis (37). We have previously shown that SPLUNC1 can inhibit ENaC from rat and human airways (11). Here, we demonstrate that S18 can also attenuate ASL absorption across murine tracheal epithelia (Fig. 7, *A* and *B*). These data suggest that at least in higher organisms, there are minimal species differences in S18's efficacy and that rodents can be used to model S18's pharmacodynamics. Since S18 is an ENaC-binding peptide, we hypothesized *1*) that it does not cross the airway epithelia and *2*) that if it did, it would be rapidly degraded by proteases in the blood and/or the proximal tubule (43) before it could have access to ENaC in the distal nephron. Indeed, despite adding S18 at a very high level intratracheally (100 mM), only ~10 millionth of this (i.e., 1.5 nM) was detected in serum, suggesting favorable pharmacodynamics (Fig. 7, *E* and *F*). Our metabolic cage data were consistent with these observations since intraperitoneal injection of S18 did not induce diuresis, natriuresis, or antikaliuresis in conscious mice, which was in contrast to an equimolar dose of amiloride (Fig. 5). An alternative explanation for these observations is that since S18 is a peptide, it might have been retained in the peritoneum and was thus unavailable to inhibit ENaC in the distal nephron. Thus, to address this concern, we also infused S18 directly into the bloodstream of anesthetized rats. In these studies, we also found that S18 had no significant effect on any renal parameters, including urine flow rate, Na^+ excretion, and, most notably, K^+ retention (Fig. 6 and Table 1). Again, these data were in sharp contrast to an equimolar dose of amiloride, which induced significant natriuresis, diuresis, and increased serum K^+ levels due to decreased urinary K^+ excretion (Fig. 6). On the basis of these data, we propose that inhaled, S18 would be better tolerated by patients than small molecules because of the absence of renal toxicity.

To determine the therapeutic efficacy in vivo, we tested the ability of S18 to reduce neonatal mortality in the β-ENaC-Tg mouse model of CF (54). To confirm that S18 was functional in mice, we first exposed tracheal epithelial cultures from wild-type or β-ENaC-Tg mice to S18. Using this approach, we found that S18 increased ASL height for both phenotypes (Fig. 7, *A* and *B*). Vehicle-treated β-ENaC-Tg pups displayed significant mortality, and amiloride treatment showed no improvement in overall mortality. However, we found that S18 treatment resulted in an ~46% decrease in pulmonary mortality at PND 14 (Fig. 7*C*). Zhou et al. (54) previously reported that amiloride reduced pulmonary mortality of β-ENaC-Tg pups by ~70% following amiloride treatment. These divergent effects of amiloride were likely the result of differences in genetic backgrounds of the β-ENaC-Tg mice used in each study: mortality of neonatal β-ENaC-Tg mice is strongly affected by genetic background and ranges from ~100 to 20% depending on the strain used, with neonatal mortality closely correlating with the presence of asphyxiating mucus plugs (28). Since S18 freely penetrates mucus (Fig. 2), we chose to use mice on the plugging-prone, high-mortality (~100% mortality at PND 14) FVB/NJ:C57BL/6N genetic background in our studies. In contrast, the mice used in the Zhou et al. study were on a much milder mixed C3H:C57BL/6N genetic background (~50% mortality at PND 14; 54). We speculate that amiloride's inability to modulate pulmonary mortality in the more severe phenotype stems from its lower potency and shorter duration of action on airway surfaces compared with S18. This conclusion

is supported by our finding that S18 but not amiloride reduced ASL absorption (Fig. 4, *A* and *B*).

In addition to survival, we also monitored differences in growth between the treatment groups throughout the 14-day study (Fig. 7*D*). Here, we found that repeated exposure to S18 did not cause a loss of body mass. In fact, we found that preventive S18 treatment was associated with a small but significant increase in growth of the β-ENaC-Tg mice relative to vehicle. This finding was similar to that reported with hypertonic saline, providing further evidence that rehydration of the airways is associated with better survival outcomes (13). Indeed, the energy expenditure required for breathing for patients with chronic lung disease is far greater than that in normal subjects (4, 49), so it is likely that ameliorating chronic lung disease decreases this energy burden and allows the mice to gain weight (Fig. 7*D*). Given that the majority of CF patients are underweight (4), such a predicted weight gain would be beneficial. Furthermore, the growth retardation seen in the amiloride group was likely the result of ENaC blockade in the kidney and subsequent natriuresis and diuresis. This conclusion is supported by our renal studies (Figs. 4–5) and also by previous work showing that amiloride is absorbed across the airway epithelium, where it can exert its diuretic effects (17, 54).

Mucus stasis is a key pathophysiological consequence of CFTR dysfunction (15, 29). Intubated sheep provide a useful model to study mucus clearance since nebulization of CFTR(inh)-172 results in a pronounced depression of TMV, a surrogate marker of mucocilliary clearance. Following CFTR inhibition, we demonstrated that a single dose of S18 was able to restore TMV to ~93% of baseline and that unlike amiloride, this effect persisted for up to 8 h after treatment (Fig. 8). This finding also provides further evidence that inhibition of ENaC alone is able to restore normal mucus clearance in the face of continued CFTR dysfunction.

In conclusion, our data indicate that S18 is a promising therapeutic candidate that *1*) does not interact with mucus/mucins; *2*) results in a more durable inhibition of ENaC than amiloride; *3*) is associated with a sustained restoration of mucus clearance in sheep; and *4*) decreased morbidity and mortality in the β-ENaC-Tg mouse. Importantly, we also demonstrate that S18 does not induce any significant renal side effects, likely because of extremely low bioavailability in the blood after inhalation. S18 is the naturally occurring 18-residue peptide that is directly homologous to SPLUNC1's NH_2-terminal ENaC inhibitory domain (18). To the best of our knowledge, S18 is the first naturally occurring peptide to have the potential to successfully rehydrate the airways and improve mucus clearance without simultaneously causing hyperkalemia as a result of renal ENaC inhibition. Taken together, these data indicate that S18 may be a suitable candidate to be inhaled via nebulizers for the treatment of CF lung disease.

ACKNOWLEDGMENTS

The help of the University of North Carolina (UNC) Cystic Fibrosis Center Tissue Culture Core is gratefully acknowledged. We thank Drs. Krzysztof Krajewski and Brian Stahl from UNC's High-Throughput Peptide Synthesis and Array Facility for generating the peptides. We also thank Dr. Nicholas Moss for critical input into the renal experiments and Dr. David Hill for personally supplying mucus.

GRANTS

This study was supported by the North Carolina Biotechnology Center; National Institutes of Health Grants HL-108927, HL-1108723, HL-103940, P30-DK-065988, DK-051870, and GM-000678; and Cystic Fibrosis Foundation Grant BOUCHE15RO.

DISCLOSURES

S. T. Terryah, R. C. Fellner, D. W. Scott, J. I. Sesma, and R. Tarran have equity in Spyryx Biosciences. The other authors have no financial disclosures.

AUTHOR CONTRIBUTIONS

S.T.T., R.C.F., S.A., B.R., J.I.S., S.H.R., M.K., W.M.A., W.J.A., and R.T. conceived and designed research; S.T.T., R.C.F., S.A., P.J.M., B.R., J.I.S., C.S.K., A.L.G., D.W.S., J.R.S., J.C., M.K., and R.T. performed experiments; S.T.T., R.C.F., S.A., P.J.M., B.R., J.I.S., C.S.K., A.L.G., D.W.S., J.R.S., J.C., M.K., W.M.A., W.J.A., and R.T. analyzed data; S.T.T., R.C.F., P.J.M., B.R., C.S.K., A.L.G., D.W.S., J.R.S., J.C., S.H.R., M.K., W.M.A., W.J.A., and R.T. interpreted results of experiments; S.T.T., R.C.F., S.A., P.J.M., B.R., and R.T. prepared figures; S.T.T. and R.T. drafted manuscript; S.T.T., R.C.F., S.A., and R.T. edited and revised manuscript; S.T.T., R.C.F., S.A., P.J.M., B.R., J.I.S., C.S.K., A.L.G., D.W.S., J.R.S., J.C., S.H.R., M.K., W.M.A., W.J.A., and R.T. approved final version of manuscript.

REFERENCES

1. **Ahmad S, Tyrrell J, Walton WG, Tripathy A, Redinbo MR, Tarran R.** Short palate, lung, and nasal epithelial clone 1 has antimicrobial and antibiofilm activities against the *Burkholderia cepacia* complex. *Antimicrob Agents Chemother* 60: 6003–6012, 2016. doi:10.1128/AAC.00975-16.
2. **App EM, King M, Helfesrieder R, Köhler D, Matthys H.** Acute and long-term amiloride inhalation in cystic fibrosis lung disease. A rational approach to cystic fibrosis therapy. *Am Rev Respir Dis* 141: 605–612, 1990. doi:10.1164/ajrccm/141.3.605.
3. **Åstrand AB, Hemmerling M, Root J, Wingren C, Pesic J, Johansson E, Garland AL, Ghosh A, Tarran R.** Linking increased airway hydration, ciliary beating, and mucociliary clearance through ENaC inhibition. *Am J Physiol Lung Cell Mol Physiol* 308: L22–L32, 2015. doi:10.1152/ajplung.00163.2014.
4. **Bell SC, Saunders MJ, Elborn JS, Shale DJ.** Resting energy expenditure and oxygen cost of breathing in patients with cystic fibrosis. *Thorax* 51: 126–131, 1996. doi:10.1136/thx.51.2.126.
5. **Boucher RC, Cotton CU, Gatzy JT, Knowles MR, Yankaskas JR.** Evidence for reduced Cl^- and increased Na^+ permeability in cystic fibrosis human primary cell cultures. *J Physiol* 405: 77–103, 1988. doi:10.1113/jphysiol.1988.sp017322.
6. **Bove PF, Grubb BR, Okada SF, Ribeiro CM, Rogers TD, Randell SH, O'Neal WK, Boucher RC.** Human alveolar type II cells secrete and absorb liquid in response to local nucleotide signaling. *J Biol Chem* 285: 34939–34949, 2010. doi:10.1074/jbc.M110.162933.
7. **Britto CJ, Cohn L.** Bactericidal/permeability-increasing protein fold-containing family member A1 in airway host protection and respiratory disease. *Am J Respir Cell Mol Biol* 52: 525–534, 2015. doi:10.1165/rcmb.2014-0297RT.
8. **Burrows E, Southern KW, Noone P.** Sodium channel blockers for cystic fibrosis. *Cochrane Database Syst Rev* 3: CD005087, 2006. doi:10.1002/14651858.CD005087.pub2.
9. **Coin I, Beyermann M, Bienert M.** Solid-phase peptide synthesis: from standard procedures to the synthesis of difficult sequences. *Nat Protoc* 2: 3247–3256, 2007. doi:10.1038/nprot.2007.454.
10. **Donaldson SH, Corcoran TE, Laube BL, Bennett WD.** Mucociliary clearance as an outcome measure for cystic fibrosis clinical research. *Proc Am Thorac Soc* 4: 399–405, 2007. doi:10.1513/pats.200703-042BR.
11. **Garcia-Caballero A, Rasmussen JE, Gaillard E, Watson MJ, Olsen JC, Donaldson SH, Stutts MJ, Tarran R.** SPLUNC1 regulates airway surface liquid volume by protecting ENaC from proteolytic cleavage. *Proc Natl Acad Sci USA* 106: 11412–11417, 2009. [Erratum in *Proc Natl Acad Sci USA* 106(35): 15091, 2009. doi:10.1073/pnas.0908688106.]. doi:10.1073/pnas.0903609106.
12. **Garland AL, Walton WG, Coakley RD, Tan CD, Gilmore RC, Hobbs CA, Tripathy A, Clunes LA, Bencharit S, Stutts MJ, Betts L, Redinbo MR, Tarran R.** Molecular basis for pH-dependent mucosal dehydration

in cystic fibrosis airways. *Proc Natl Acad Sci USA* 110: 15973–15978, 2013. doi:10.1073/pnas.1311999110.

13. **Graeber SY, Zhou-Suckow Z, Schatterny J, Hirtz S, Boucher RC, Mall MA.** Hypertonic saline is effective in the prevention and treatment of mucus obstruction, but not airway inflammation, in mice with chronic obstructive lung disease. *Am J Respir Cell Mol Biol* 49: 410–417, 2013. doi:10.1165/rcmb.2013-0050OC.
14. **Graham A, Hasani A, Alton EW, Martin GP, Marriott C, Hodson ME, Clarke SW, Geddes DM.** No added benefit from nebulized amiloride in patients with cystic fibrosis. *Eur Respir J* 6: 1243–1248, 1993.
15. **Haq IJ, Gray MA, Garnett JP, Ward C, Brodlie M.** Airway surface liquid homeostasis in cystic fibrosis: pathophysiology and therapeutic targets. *Thorax* 71: 284–287, 2016. doi:10.1136/thoraxjnl-2015-207588.
16. **Hirsh AJ.** Altering airway surface liquid volume: inhalation therapy with amiloride and hyperosmotic agents. *Adv Drug Deliv Rev* 54: 1445–1462, 2002. doi:10.1016/S0169-409X(02)00161-8.
17. **Hirsh AJ, Sabater JR, Zamurs A, Smith RT, Paradiso AM, Hopkins S, Abraham WM, Boucher RC.** Evaluation of second generation amiloride analogs as therapy for cystic fibrosis lung disease. *J Pharmacol Exp Ther* 311: 929–938, 2004. doi:10.1124/jpet.104.071886.
18. **Hobbs CA, Blanchard MG, Alijevic O, Tan CD, Kellenberger S, Bencharit S, Cao R, Kesimer M, Walton WG, Henderson AG, Redinbo MR, Stutts MJ, Tarran R.** Identification of the SPLUNC1 ENaC-inhibitory domain yields novel strategies to treat sodium hyperabsorption in cystic fibrosis airway epithelial cultures. *Am J Physiol Lung Cell Mol Physiol* 305: L990–L1001, 2013. doi:10.1152/ajplung.00103.2013.
19. **Hobbs CA, Da Tan C, Tarran R.** Does epithelial sodium channel hyperactivity contribute to cystic fibrosis lung disease? *J Physiol* 591: 4377–4387, 2013. doi:10.1113/jphysiol.2012.240861.
20. **Jiang D, Wenzel SE, Wu Q, Bowler RP, Schnell C, Chu HW.** Human neutrophil elastase degrades SPLUNC1 and impairs airway epithelial defense against bacteria. *PLoS One* 8: e64689, 2013. doi:10.1371/journal.pone.0064689.
21. **Kerem E, Bistritzer T, Hanukoglu A, Hofmann T, Zhou Z, Bennett W, MacLaughlin E, Barker P, Nash M, Quittell L, Boucher R, Knowles MR.** Pulmonary epithelial sodium-channel dysfunction and excess airway liquid in pseudohypoaldosteronism. *N Engl J Med* 341: 156–162, 1999. doi:10.1056/NEJM199907153410304.
22. **Kesimer M, Kirkham S, Pickles RJ, Henderson AG, Alexis NE, Demaria G, Knight D, Thornton DJ, Sheehan JK.** Tracheobronchial air-liquid interface cell culture: a model for innate mucosal defense of the upper airways? *Am J Physiol Lung Cell Mol Physiol* 296: L92–L100, 2009. doi:10.1152/ajplung.90388.2008.
23. **Kesimer M, Sheehan JK.** Analyzing the functions of large glycoconjugates through the dissipative properties of their absorbed layers using the gel-forming mucin MUC5B as an example. *Glycobiology* 18: 463–472, 2008. doi:10.1093/glycob/cwn024.
24. **Knowles MR, Church NL, Waltner WE, Yankaskas JR, Gilligan P, King M, Edwards LJ, Helms RW, Boucher RC.** A pilot study of aerosolized amiloride for the treatment of lung disease in cystic fibrosis. *N Engl J Med* 322: 1189–1194, 1990. doi:10.1056/NEJM199004263221704.
25. **Köhler D, App E, Schmitz-Schumann M, Würtemberger G, Matthys H.** Inhalation of amiloride improves the mucociliary and the cough clearance in patients with cystic fibroses. *Eur J Respir Dis Suppl* 146: 319–326, 1986.
26. **Lai SK, Wang YY, Wirtz D, Hanes J.** Micro- and macrorheology of mucus. *Adv Drug Deliv Rev* 61: 86–100, 2009. doi:10.1016/j.addr.2008.09.012.
27. **Liu Y, Di ME, Chu HW, Liu X, Wang L, Wenzel S, Di YP.** Increased susceptibility to pulmonary *Pseudomonas* infection in Splunc1 knockout mice. *J Immunol* 191: 4259–4268, 2013. doi:10.4049/jimmunol.1202340.
28. **Livraghi-Butrico A, Grubb BR, Kelly EJ, Wilkinson KJ, Yang H, Geiser M, Randell SH, Boucher RC, O'Neal WK.** Genetically determined heterogeneity of lung disease in a mouse model of airway mucus obstruction. *Physiol Genomics* 44: 470–484, 2012. doi:10.1152/physiolgenomics.00185.2011.
29. **Livraghi A, Randell SH.** Cystic fibrosis and other respiratory diseases of impaired mucus clearance. *Toxicol Pathol* 35: 116–129, 2007. doi:10.1080/01926230601060025.
30. **Ma T, Thiagarajah JR, Yang H, Sonawane ND, Folli C, Galietta LJ, Verkman AS.** Thiazolidinone CFTR inhibitor identified by high-throughput screening blocks cholera toxin-induced intestinal fluid secretion. *J Clin Invest* 110: 1651–1658, 2002. doi:10.1172/JCI0216112.
31. **MacLean B, Tomazela DM, Shulman N, Chambers M, Finney GL, Frewen B, Kern R, Tabb DL, Liebler DC, MacCoss MJ.** Skyline: an open source document editor for creating and analyzing targeted proteomics experiments. *Bioinformatics* 26: 966–968, 2010. doi:10.1093/bioinformatics/btq054.
32. **Mall M, Grubb BR, Harkema JR, O'Neal WK, Boucher RC.** Increased airway epithelial Na^+ absorption produces cystic fibrosis-like lung disease in mice. *Nat Med* 10: 487–493, 2004. doi:10.1038/nm1028.
33. **Mall MA, Button B, Johannesson B, Zhou Z, Livraghi A, Caldwell RA, Schubert SC, Schultz C, O'Neal WK, Pradervand S, Hummler E, Rossier BC, Grubb BR, Boucher RC.** Airway surface liquid volume regulation determines different airway phenotypes in liddle compared with βENaC-overexpressing mice. *J Biol Chem* 285: 26945–26955, 2010. doi:10.1074/jbc.M110.151803.
34. **Matalon S, Bartoszewski R, Collawn JF.** Role of epithelial sodium channels in the regulation of lung fluid homeostasis. *Am J Physiol Lung Cell Mol Physiol* 309: L1229–L1238, 2015. doi:10.1152/ajplung.00319.2015.
35. **Matsui H, Grubb BR, Tarran R, Randell SH, Gatzy JT, Davis CW, Boucher RC.** Evidence for periciliary liquid layer depletion, not abnormal ion composition, in the pathogenesis of cystic fibrosis airways disease. *Cell* 95: 1005–1015, 1998. doi:10.1016/S0092-8674(00)81724-9.
36. **O'Riordan TG, Donn KH, Hodsman P, Ansede JH, Newcomb T, Lewis SA, Flitter WD, White VS, Johnson MR, Montgomery AB, Warnock DG, Boucher RC.** Acute hyperkalemia associated with inhalation of a potent ENaC antagonist: phase 1 trial of GS-9411. *J Aerosol Med Pulm Drug Deliv* 27: 200–208, 2014. doi:10.1089/jamp.2013.1037.
37. **Perazella MA.** Drug-induced hyperkalemia: old culprits and new offenders. *Am J Med* 109: 307–314, 2000. doi:10.1016/S0002-9343(00)00496-4.
38. **Puchelle E, Bajolet O, Abély M.** Airway mucus in cystic fibrosis. *Paediatr Respir Rev* 3: 115–119, 2002. doi:10.1016/S1526-0550(02)00005-7.
39. **Radicioni G, Cao R, Carpenter J, Ford AA, Wang T, Li L, Kesimer M.** The innate immune properties of airway mucosal surfaces are regulated by dynamic interactions between mucins and interacting proteins: the mucin interactome. *Mucosal Immunol* 9: 1442–1454, 2016. doi:10.1038/mi.2016.27.
40. **Riordan JR.** CFTR function and prospects for therapy. *Annu Rev Biochem* 77: 701–726, 2008. doi:10.1146/annurev.biochem.75.103004.142532.
41. **Rollins BM, Garcia-Caballero A, Stutts MJ, Tarran R.** SPLUNC1 expression reduces surface levels of the epithelial sodium channel (ENaC) in *Xenopus laevis* oocytes. *Channels (Austin)* 4: 255–259, 2010. doi:10.4161/chan.4.4.12255.
42. **Sayeed S, Nistico L, St Croix C, Di YP.** Multifunctional role of human SPLUNC1 in *Pseudomonas aeruginosa* infection. *Infect Immun* 81: 285–291, 2013. doi:10.1128/IAI.00500-12.
43. **Scherberich JE, Wolf G, Stuckhardt C, Kugler P, Schoeppe W.** Characterization and clinical role of glomecular and tubular proteases from human kidney. In: *Proteases II: Potential Role in Health and Disease*, edited by Hörl WH and Heidland A. Boston, MA: Springer, 1988, p. 275–282. doi:10.1007/978-1-4613-1057-0_32.
44. **Tarran R, Boucher RC.** Thin-film measurements of airway surface liquid volume/composition and mucus transport rates in vitro. *Methods Mol Med* 70: 479–492, 2002. doi:10.1385/1-59259-187-6:479.
45. **Tarran R, Button B, Picher M, Paradiso AM, Ribeiro CM, Lazarowski ER, Zhang L, Collins PL, Pickles RJ, Fredberg JJ, Boucher RC.** Normal and cystic fibrosis airway surface liquid homeostasis. The effects of phasic shear stress and viral infections. *J Biol Chem* 280: 35751–35759, 2005. doi:10.1074/jbc.M505832200.
46. **Tarran R, Grubb BR, Parsons D, Picher M, Hirsh AJ, Davis CW, Boucher RC.** The CF salt controversy: in vivo observations and therapeutic approaches. *Mol Cell* 8: 149–158, 2001. doi:10.1016/S1097-2765(01)00286-6.
47. **Tarran R, Redinbo MR.** Mammalian short palate lung and nasal epithelial clone 1 (SPLUNC1) in pH-dependent airway hydration. *Int J Biochem Cell Biol* 52: 130–135, 2014. doi:10.1016/j.biocel.2014.03.002.
48. **Thibodeau PH, Butterworth MB.** Proteases, cystic fibrosis and the epithelial sodium channel (ENaC). *Cell Tissue Res* 351: 309–323, 2013. doi:10.1007/s00441-012-1439-z.
49. **Vaisman N, Pencharz PB, Corey M, Canny GJ, Hahn E.** Energy expenditure of patients with cystic fibrosis. *J Pediatr* 111: 496–500, 1987. doi:10.1016/S0022-3476(87)80107-5.
50. **Walton WG, Ahmad S, Little MS, Kim CS, Tyrrell J, Lin Q, Di YP, Tarran R, Redinbo MR.** Structural features essential to the antimicrobial

functions of human SPLUNC1. *Biochemistry* 55: 2979–2991, 2016. doi:10.1021/acs.biochem.6b00271.

51. **Worlitzsch D, Tarran R, Ulrich M, Schwab U, Cekici A, Meyer KC, Birrer P, Bellon G, Berger J, Weiss T, Botzenhart K, Yankaskas JR, Randell S, Boucher RC, Döring G.** Effects of reduced mucus oxygen concentration in airway *Pseudomonas* infections of cystic fibrosis patients. *J Clin Invest* 109: 317–325, 2002. doi:10.1172/JCI0213870.
52. **Worthington EN, Tarran R.** Methods for ASL measurements and mucus transport rates in cell cultures. *Methods Mol Biol* 742: 77–92, 2011. doi:10.1007/978-1-61779-120-8_5.
53. **Zhou Z, Duerr J, Johannesson B, Schubert SC, Treis D, Harm M, Graeber SY, Dalpke A, Schultz C, Mall MA.** The ENaC-overexpressing mouse as a model of cystic fibrosis lung disease. *J Cyst Fibros* 10, *Suppl* 2: S172–S182, 2011. doi:10.1016/S1569-1993(11)60021-0.
54. **Zhou Z, Treis D, Schubert SC, Harm M, Schatterny J, Hirtz S, Duerr J, Boucher RC, Mall MA.** Preventive but not late amiloride therapy reduces morbidity and mortality of lung disease in βENaC-overexpressing mice. *Am J Respir Crit Care Med* 178: 1245–1256, 2008. doi:10.1164/rccm.200803-442OC.